Inorganica Chimica Acta, *204* (1993) 199–212

A spectrophotometric and ESR study of monomer, μ-oxo dimer, di(μ-oxo) dimer interconversion of nitridotechnetium(VI) complexes in solutions of sulfur and phosphorus oxo acids

John Baldas, John F. Boas, Zlata Ivanov
Australian Radiation Laboratory, Lower Plenty Road, Yallambie, Vic. 3085 (Australia)

and Bruce D. James
Department of Chemistry, La Trobe University, Bundoora, Vic. 3083 (Australia)

(Received September 10, 1992)

Abstract

UV–Vis and ESR spectroscopy have been used to study the behaviour of $Cs_2[TcNCl_5]$ and the hydrolysis product $[\{TcN(OH)(OH_2)\}_2(\mu\text{-}O)_2]$ (**1**) in concentrated and aqueous solutions of a variety of sulfur and phosphorus oxo acids ranging from the very weakly coordinating CF_3SO_3H to H_2SO_4 and the coordinating acids H_3PO_4 and $H_4P_2O_7$. The paramagnetic monomeric $Tc^{VI}N^{3+}$ (d^1) forms were readily identified by ESR spectroscopy and the diamagnetic dimeric μ-oxo ($Tc_2N_2O^{4+}$) and di(μ-oxo) ($Tc_2N_2O_2^{2+}$) forms by their UV–Vis spectra. For solutions of $Cs_2[TcNCl_5]$ the chemical form of $Tc^{VI}N$ and the rate of the conversion of monomer → μ-oxo dimer → di(μ-oxo) dimer is dependent on the presence of Cl^- and the concentration and complexing ability of the acid, with the monomeric form being favoured by the acids of greater complexing power. For solutions of **1** the reverse order of conversion was observed. In 1 M CF_3SO_3H, $MeSO_3H$ or toluene-*p*-sulfonic acid, **1** is converted to the di(μ-oxo) aquanitrido cation $[\{TcN(OH_2)_3\}_2(\mu\text{-}O)_2]^{2+}$ while in 7.5 M CF_3SO_3H it is proposed that the predominant form is the μ-oxo aqua dimer $[\{TcN(OH_2)_4\}_2(\mu\text{-}O)]^{4+}$. In H_2SO_4 and the phosphorus oxo acids the aqua cations are coordinated by the acid anions. The monomeric aqua cation, $[TcN(OH_2)_5]^{3+}$, does not appear to be a viable species, as is also the case for MoO^{3+}(aq), and spontaneously dimerises in 7.5 M CF_3SO_3H. In anhydrous CF_3SO_3H or H_2SO_4 monomeric $Tc^{VI}N$ with $CF_3SO_3^-$ or HSO_4^- coordination is observed. A characteristic feature of the UV–Vis spectra of monomeric $Tc^{VI}N$ is a strong absorption at 266–300 nm assigned to $\pi N \rightarrow Tc$ charge transfer. The μ-oxo dimers show an intense visible absorption at 470–510 nm.

Introduction

Monomeric and dimeric oxo complexes are a characteristic and dominant feature of the chemistry of Mo^V. Complexes containing the monomeric MoO^{3+} and the dimeric $[Mo_2O_3]^{4+}$ and $[Mo_2O_4]^{2+}$ cores have been extensively studied and many have been structurally characterised [1–3]. We have recently reported that the chemistry of $Tc^{VI}N$ closely parallels that of the isoelectronic Mo^VO [4]. Five- and six-coordinated monomeric technetium species are exemplified by $AsPh_4[TcNX_4]$ [5] and $NEt_4[TcNX_4(OH_2)]$ (X = Cl, Br) [6] and the two $Tc^{VI}N$ dimeric cores A and B have been crystallographically established in the cyclic tetramer $(AsPh_4)_4[Tc_4N_4(O)_2(ox)_6]$ (ox = oxalate(2−)) [7] and in $[\{TcN(S_2CNR_2)\}_2(\mu\text{-}O)_2]$ (R = Et or $R_2 = (CH_2)_4$), respectively [8]. The di(μ-oxo) core B may also occur in the six-coordinate form with an additional ligand *trans* to each nitrido ligand, but to date all isolated complexes have been found to be five-coordinate. The bridging oxo ligand in A is *cis* to the nitrido ligands, as expected on the basis of bonding considerations for d^1–d^1 OM–O–MO systems [1] and the isoelectronic nature of the O^{2-} and N^{3-} ligands. This is in contrast to the d^2–d^2 $Tc^V_2O_3$ dimers where the O=Tc–O–Tc=O system is linear or near linear [9].

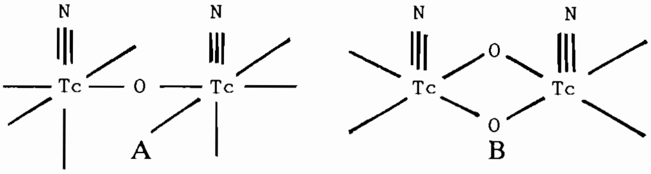

The study of the chemistry of technetium has been greatly stimulated by the use of the short lived ^{99m}Tc

radionuclide ($t_{1/2}=6.01$ h) in diagnostic nuclear medicine and the availability of the long-lived ^{99}Tc ($t_{1/2}=2.12\times10^5$ years) for conventional chemical work. $[^{99m}TcNCl_4]^-$ has been developed as an agent for the preparation of ^{99m}TcN-radiopharmaceuticals [10]. A knowledge of the behaviour of $[TcNCl_4]^-$ in aqueous coordinating media is essential for further developments in this field.

It is of particular interest to note that technetium in the +6 oxidation state is the only transition metal known to form oxygen-bridged nitrido complexes or an aquanitrido cation. The $Tc^{VI}\equiv N$ bond is highly stable to acid hydrolysis, a property demonstrated by the preparative method for $[TcNX_4]^-$ (X = Cl, Br), which involves reflux in conc. HX [5]. By way of contrast a considerable number of $Tc^{V}N$ complexes have been prepared and structurally characterised and all have been found to be monomeric.

Dissolution of $Cs_2[TcNCl_5]$ in water has been shown to result in hydrolysis to a brown precipitate of '$TcN(OH)_3$', analogous to '$MoO(OH)_3$', which has been formulated as the dimeric $[\{TcN(OH)(OH_2)\}_2(\mu\text{-}O)_2]$ (**1**) (or alternatively as the polymeric $[TcN(OH)(OH_2)(\mu\text{-}O)]_n$ or $[TcN(OH)(\mu\text{-}O)]_n\cdot nH_2O$ [4]. This precipitate readily dissolves in solutions of weakly coordinating acids, such as toluene-*p*-sulfonic (Hpts) or CF_3SO_3H, to give the aquanitrido cation $[\{Tc^{VI}N(OH_2)_3\}_2(\mu\text{-}O)_2]^{2+}$ (core B with six-coordination) [11], which is the isoelectronic analogue of the well-established $[Mo^{V}{}_2O_4(OH_2)_6]^{2+}$ aqua cation [12].

We now report a study of complex formation and the interconversion of monomeric and dimeric $Tc^{VI}N$ cores in concentrated and aqueous solutions of a variety of sulfur and phosphorus oxo acids. UV–Vis spectroscopy is used to identify the singly and doubly oxygen bridged species and the paramagnetic monomeric species are easily and reliably identified by ESR spectroscopy. Previous studies of ligand exchange of $Tc^{VI}N$ systems in organic solvents have involved only monomeric $Tc^{VI}N$ species [13].

Experimental

All reagents and acids used were of analytical grade or the highest available commercial purity. The 85% phosphoric acid used was found to be 17.5 M by titration against standard base. Pyrophosphoric acid solutions were prepared immediately before use by the addition of crushed ice to the solid $H_4P_2O_7$ to minimise the temperature rise during dissolution and the hydrolysis to H_3PO_4. The preparation of $Cs_2[TcNCl_5]$ has been described previously [14]. The purity was checked by Tc analysis (calc. 17.8, found 17.8%). The brown precipitate of $[\{TcN(OH)(OH_2)\}_2(\mu\text{-}O)_2]$ (**1**) was prepared by the hydrolysis of $Cs_2[TcNCl_5]$ and separation of the solid by centrifugation. After removal of the supernate the solid was resuspended in water and recentrifuged. Since the hydrolysis and washing steps resulted in some loss of technetium in the supernate, an aliquot of the solution of **1** in each acid was decolourised by the addition of H_2O_2 and the technetium content determined by liquid scintillation counting.

UV–Vis spectra were measured in 1 cm or 2 mm cells on a Varian DMS 300 spectrophotometer with a microcomputer system for the collection of multiple scans at fixed time intervals. Unless otherwise stated the $Cs_2[TcNCl_5]$ solutions were 4×10^{-4} M and the solutions of **1** in the range 2.7×10^{-4} to 8.5×10^{-4} M (the exact Tc content was determined as above). Molar absorption coefficient (ϵ) values are quoted in units of M^{-1} cm^{-1}. FT-IR spectra (4000–250 cm^{-1}) were determined in KBr disks on a Digilab FTS7 spectrophotometer.

Paper electrophoresis was performed (at 600 V unless otherwise stated) on a Camag high voltage system using 2×44 cm Whatman No. 1 paper strips. An air pressure-bag system was used to ensure intimate contact of the paper strips and the thermally conductive supporting surface, which was cooled by the circulation of chilled water (~10 °C). Efficient cooling is essential since 30–50 W of heat may be generated in a single paper strip with 0.5 M of a strong acid as the supporting electrolyte. After separation, the paper strips were dried and the technetium distribution determined by a radiochromatogram scanner.

ESR spectroscopy

ESR spectra were recorded at 130 K using a Bruker ESR-200D-SRC spectrometer and associated equipment. Spectral simulations were performed on a Data General MV8000 computer using the programs described previously which employ the standard second-order perturbation theory expressions for the magnetic fields and transition probabilities [15]. The spin Hamiltonian used to represent the spectra was of the form

$$\mathscr{H}=g_{\parallel}\beta B_zS_z+g_{\perp}\beta(B_xS_x+B_yS_y)+A_{\parallel}S_zI_z$$
$$+A_{\perp}(S_xI_x+S_yI_y)+Q[I^2{}_z-I(I+1)/3]+\mathscr{H}_{\rm shf}$$

where $S=1/2$, $I=9/2$ for the Tc^{VI} ion and the other symbols have their usual meanings.

For ESR studies all the $Cs_2[TcNCl_5]$ solutions were 2×10^{-3} M and the solutions of **1** in the range 1.4×10^{-3} to 1.8×10^{-3} M. Comparisons of the signal intensity corresponding to the various ESR detectable species were made by comparing the height × (peak-to-peak width)^2 of the highest field perpendicular lines, recorded as the derivative of the absorption. The standard spectrum was that of 2×10^{-3} M $Cs_2[TcNCl_5]$ in conc. HCl, where it is assumed that all the Tc in solution is present as the $[TcNCl_4]^-$ anion. Intensity comparison could be made to an accuracy of ±10%.

Analysis of the spectra by means of computer simulation is the most accurate means of determining the g and A values and hence of differentiating between different species. In the present case, as a consequence of the high value of I for Tc (9/2) and the large value of A, the position of the lowest field 'parallel' line is also a useful indicator of which species are present. For this reason, and because in some cases the g and A values are quite similar, the position of the lowest field 'parallel' line is also given in Tables 1–3 which list the spin Hamiltonian parameters for the systems discussed in this paper.

Results and discussion

The most useful compounds for the study of $Tc^{VI}N$ aqueous solution chemistry are $Cs_2[TcNCl_5]$ and its hydrolysis product $[\{TcN(OH)(OH_2)\}_2(\mu\text{-}O)_2]$ (**1**), both of which are soluble in a wide variety of organic and inorganic acids. The use of **1** is particularly advantageous since it allows complex formation to be studied in the absence of competition from chloride ion. Thus, for example, while the ESR spectrum of a solution of **1** in 50% HF (28.6 M) showed the presence of only $[TcNF_4]^-$, a HF solution of $Cs_2[TcNCl_5]$ contained all of the $[TcNF_nCl_{(4-n)}]^-$ ($n=0$–4) species [15]. The chloro ligands of $[TcNCl_5]^{2-}$ are labile, with the strong *trans* influence of the nitrido ligand resulting in the *trans* chloride being the most easily replaced. ESR studies have shown no evidence for the presence of $[TcNCl_5]^{2-}$ in conc. HCl solution [16] (cf. in conc. HCl Mo^VO exists as $[MoOCl_5]^{2-}$ [1]) and the isolation of $NEt_4[TcNCl_4(OH_2)]$ [6] suggests that the form in this medium is $[TcNCl_4(OH_2)]^-$ (henceforth the anion of $Cs_2[TcNCl_5]$ in acid solution will be written simply as $[TcNCl_4]^-$). The equatorial chloro ligands in $[TcNCl_5]^{2-}$ are also readily replaced. Solutions of $Cs_2[TcNCl_5]$ in 47% HBr rapidly turn blue and the ESR spectrum shows the presence of only $[TcNBr_4]^-$, while dissolution in water results in complete hydrolysis to **1** [15].

Monomeric $Tc^{VI}N$ complexes in solution are readily detected and identified by ESR spectroscopy and this method has been extensively used for this purpose [15]. The Tc_2N_2O and $Tc_2N_2O_2$ dimers are ESR silent but UV–Vis spectroscopy offers a convenient method of distinguishing between the two forms. Studies of Mo^VO chemistry have shown that Mo_2O_3 dimers in solution exhibit intense visible absorption while the Mo_2O_4 dimers generally lack any pronounced visible absorption [1]. A strong visible absorption at ~525 nm was considered diagnostic of Mo_2O_3 complexes, but more recent results have shown this criterion to be too restrictive [17]. Complexes such as $[Mo_2O_3Cl_2(HB(pz)_3)_2]$ ($HB(pz)_3$ = hydrotris(1-pyrazolyl)borate) and $[Mo_2O_3Cl_4(dmf)_4]$ show absorptions at 462 and 461 nm, respectively, and a strong absorption at ~450 nm for $[MoOCl_5]^{2-}$ solutions in 5–6 M HCl has been attributed to $[Mo_2O_3Cl_8]^{4-}$ [18]. Data on $Tc^{VI}N$ dimers are limited but there is good evidence to support a similar generalisation. The only structurally characterised Tc_2N_2O complex is the red–purple cyclic tetramer $(AsPh_4)_4[Tc_4N_4(O)_2(ox)_6]$ which consists of two [TcN(ox)–O–TcN(ox)] units joined by two quadridentate oxalato ligands and shows an intense absorption at 493 nm ($\epsilon=39\,200$ M^{-1} cm^{-1} for the tetramer) [8]. The $Tc_2N_2O_2$ dimers $[\{TcN(S_2CNR_2)\}_2(\mu\text{-}O)_2]$ (λ_{max} 316sh nm) and $(AsPh_4)_2[\{TcN(CN)_2\}_2(\mu\text{-}O)_2]$ (λ_{max} 341 nm) are pale yellow, but reaction with sufficient HCl to cleave one of the oxygen bridges results in intense purple colours and absorptions at 544–545 and 534 nm, respectively [8]. In the following discussion where the concentration of a species is changing and an absolute ϵ value cannot be determined, the values given are based on [Tc] and are meant only as an indication of the relative concentration of a species at different times.

Studies in weakly coordinating sulfonic acids

The weakly coordinating, redox inactive and strongly acidic Hpts, CF_3SO_3H and to a lesser extent $MeSO_3H$ have found widespread use in the study of aqua ions [19]. These acids are generally preferable to $HClO_4$, which may cause oxidation, especially at higher concentrations.

Solutions of **1** ($[Tc]\sim1.7\times10^{-3}$ M) in 1 M Hpts, CF_3SO_3H and $MeSO_3H$ were initially pale orange–brown but within 30 min became a pale yellow. The UV–Vis spectra for a CF_3SO_3H solution are shown in Fig. 1. We have previously proposed that these solutions contain the dimeric di(μ-oxo) cation **2**

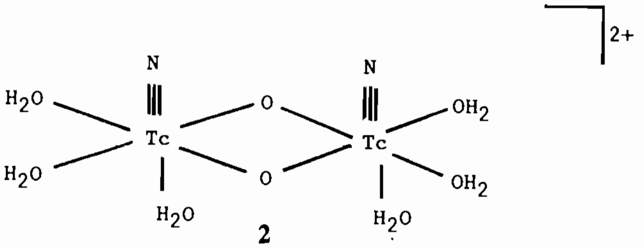

2

on the basis of electrophoretic studies, which showed the presence of a single cationic species, the isolation of $[\{TcN(S_2CNEt_2)\}_2(\mu\text{-}O)_2]$ on reaction with NaS_2CNEt_2 and the absence of ESR signals at 130 K [11]. In view of the strong *trans* influence of the nitrido

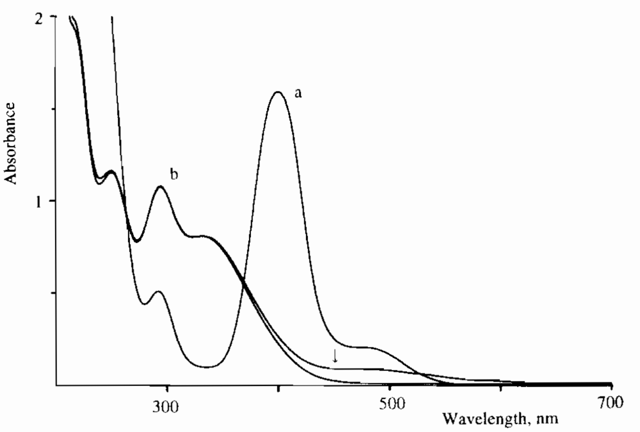

Fig. 1. UV–Vis spectra of: (a) 3.33×10^{-4} M $Cs_2[TcNCl_5]$ in 7.5 M HCl; (b) a solution of **1** in 1 M CF_3SO_3H ($[Tc]=8.35\times10^{-4}$ M) at preparation and after 4 h (time sequence is in the direction indicated by the arrow).

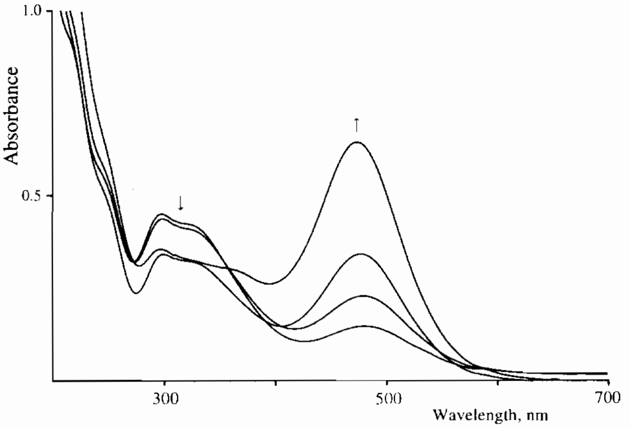

Fig. 2. UV–Vis spectra of **1** in 7.5 M CF_3SO_3H ($[Tc]=3.67\times10^{-4}$ M) at 0, 0.5, 6 and 27 h after preparation.

ligand, it is likely that the water ligands *trans* to the nitrido ligands in **2** are only weakly bound. Addition of conc. HCl (11.3 M) to a solution of **2** in any of the 1 M acids gave an intense transient purple colour and then a yellow–orange solution with the same UV–Vis spectrum as a solution of $Cs_2[TcNCl_5]$ in 7.5 M HCl (Fig. 1). The ESR spectral intensity of the latter solution corresponded to all of the Tc present.

A solution of **1** in 7.5 M CF_3SO_3H was orange and the colour deepened on standing due to the increase of the absorption initially at 481 nm but shifting to 474 nm (Fig. 2). Concomitant with this increase was the decrease of the spectrum of **2**. The absence of ESR signals is consistent with the presence of a dimeric species and the absence of monomeric forms. The absorption at 474 nm ($\epsilon > 3500$, for a dimer) is assigned to the singly oxygen-bridged cation **3**. A solution of **1** in 7.5 M $MeSO_3H$ showed similar behaviour.

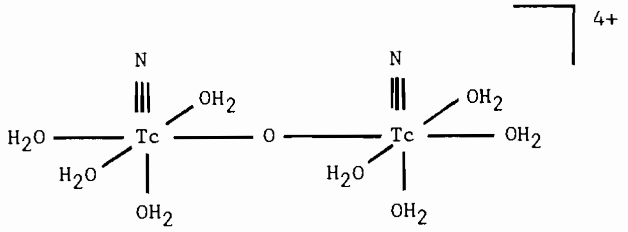

3

Solutions of **1** in anhydrous CF_3SO_3H (11.3 M) or $MeSO_3H$ (15.4 M) were initially deep red with absorptions at ~518 and 524 nm, respectively, but turned a pale brown after ~30 min. The UV–Vis spectrum of the CF_3SO_3H solution showed a strong absorption at 299 nm ($\epsilon > 12\,700$, for a monomer) which decreased in intensity on standing. The $MeSO_3H$ solution, however, exhibited a weaker broad shoulder at ~280–340 nm. On freezing to 130 K, both solutions gave ESR spectra corresponding to about 50% of the Tc present and each showed evidence for the presence of two closely related species. The spin Hamiltonian parameters are given in Table 1. In the case of CF_3SO_3H, parts of the perpendicular spectrum exhibited superhyperfine splittings of $\sim3\times10^{-4}$ cm^{-1}, presumably arising from the interaction of the unpaired electron on Tc with fluorine. The resolution of the spectrum was insufficient for the number of fluorines to be determined. The spectra in the two acids are consistent with the expected coordination through oxygen of the RSO_3^- group. In both cases signals due to $[TcNCl_4]^-$ (λ_{max} 398 nm) and corresponding to essentially all of the Tc present were restored by addition of either conc. HCl (1:1 vol./vol. to the CF_3SO_3H solution) or CsCl (40 mg/ml to the $MeSO_3H$ solution).

Solutions of $Cs_2[TcNCl_5]$ in CF_3SO_3H, $MeSO_3H$ and Hpts showed different behaviour to solutions of **1** at the same acid concentration due to competition between solvent and chloride ions for coordination to the $Tc{\equiv}N^{3+}$ core. A solution of $Cs_2[TcNCl_5]$ in anhydrous CF_3SO_3H was orange–brown. The ESR spectrum is shown in Fig. 3 and gives clear evidence for the presence of two species whose total spectral intensity corresponds to most of the Tc present. After 4 h, only one species was observed. The spectral parameters of the major species are given in Table 1 and indicate that the chloro ligands have been partially replaced by $CF_3SO_3^-$. Evidence for the coordination of $CF_3SO_3^-$ is provided by the resolution of some of the perpendicular lines of the major species into four components with a splitting of $\sim15\times10^{-4}$ cm^{-1} and an approximate intensity ratio 1:3:3:1. In contrast, the orange solution of $Cs_2[TcNCl_5]$ in $MeSO_3H$ showed signals due to $[TcNCl_4]^-$ which corresponded to most of the Tc present. The spectral intensity did not change on standing. The remainder could be accounted for by a weak spectrum indicative

TABLE 1. ESR spectral parameters for sulfonic acid solutions

System	$g_{\parallel}$ (±0.001)	$g_{\perp}$ ±0.002)	$A_{\parallel}$ (±1.0) ($\times10^4$ cm^{-1})	$A_{\perp}$ (±1.0) ($\times10^4$ cm^{-1})	Q (±1.0) ($\times10^4$ cm^{-1})	Lowest field ∥ lines
Solutions of 1 in						
CH_3SO_3H (anhyd.)	(a) 1.900	1.985	352	165	4.0	1770
	(b) 1.900	1.985	350	165	4.0	1780
CF_3SO_3H (anhyd.)	(a) 1.895	1.995	360	174	3.0	1735
	(b) 1.892	1.995	363	174	3.0	1746
	(some evidence for small fluorine shf)					
2 M Hpts	no signals observed					
Solutions of $Cs_2[TcNCl_5]$ in						
CH_3SO_3H (anhyd.)	2.0075	2.0005	293	132	4.5	1965
1 M CH_3SO_3H	similar to CF_3SO_3H (anhyd.) solution, but poorly resolved					
CF_3SO_3H (anhyd.)	(a) 1.940	1.998	332	161	4.0	1837
	superhyperfine structure due to 3 equivalent fluorines observed: $a_z=1$, $a_x \sim a_y = 15\times10^{-4}$ cm^{-1}					
2 M Hpts	(a) 1.940	1.988	328	158	4.0	1850
	(b) 1.980	1.993	310	152	4.0	1898

(a) and (b) refer to the major and minor species, respectively.

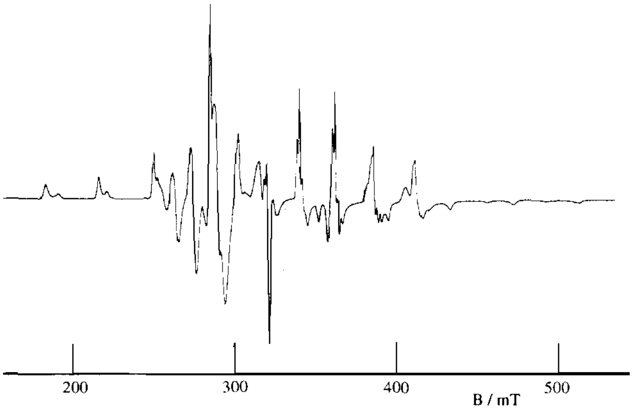

Fig. 3. ESR spectrum of 2×10^{-3} M $Cs_2[TcNCl_5]$ in anhydrous CF_3SO_3H, frozen to 130 K, 5 min after addition of the solvent. Spectrometer conditions: microwave frequency, 9.525 GHz; microwave power, 20 mW; 100 kHz modulation amplitude 0.5 mT; spectrometer gain, 2.0×10^4; recorder time constant 0.05 s; scan rate 2.0 mT/s.

of the loss of a chloro ligand. Addition of CsCl (40 mg/ml, to give a chloride concentration of ~0.25 M) resulted in the disappearance of the weak spectrum.

Considerable differences occurred between the UV–Vis spectra of the anhydrous acid solutions. The initially orange CF_3SO_3H solution changed to yellow on standing and the spectrum exhibited a maximum at ~295 nm and a maximum which shifted from 425 to 418 nm over 20 h. The intensity of the maxima increased by a factor of about 1.2 over this period. The yellow $MeSO_3H$ solution exhibited maxima at 445, 361 and 334(sh) nm, which showed only a small decrease over 20 h.

The UV–Vis spectrum of $Cs_2[TcNCl_5]$ in 7.5 M CF_3SO_3H showed only minor changes over 23 h and resembled a distorted form of the spectrum of $[TcNCl_4]^-$ in HCl with a maximum at 387 nm. The spectrum of a 2×10^{-3} M solution (2 mm cell) was similar but with the peak at 390 nm better resolved. Addition of an excess of solid CF_3SO_3Ag resulted in an immediate colour change. After removal of the precipitated AgCl by centrifugation the spectrum showed a maximum at 470 nm ($\epsilon > 5900$, for a dimer) characteristic of the singly oxygen-bridged dimer **3**. Removal of chloride thus renders the monomeric form unstable and results in a rapid dimerisation. There was no evidence of the presence of the di(μ-oxo) aqua cation **2** initially observed in the solution of **1** in 7.5 M CF_3SO_3H. The ESR spectrum of $Cs_2[TcNCl_5]$ in 7.5 M CF_3SO_3H showed only signals due to $[TcNCl_4]^-$ which did not change on standing, but the signals disappeared completely on addition of CF_3SO_3Ag. A solution of $Cs_2[TcNCl_5]$ in 5 M CF_3SO_3H showed similar behaviour with the peak at 510 nm increasing and shifting to 515 nm ($\epsilon > 6800$, for a dimer) and then decreasing after about 1 h. The spectrum did not show any obvious evidence for the presence of **2**.

A 2×10^{-3} M solution of $Cs_2[TcNCl_5]$ in 1 M CF_3SO_3H reproduced the colour changes observed in the more concentrated acids. On dissolution the yellow colour turned to a claret-red after a few seconds and then faded to a pale yellow–brown. The claret-red solution gave poorly resolved ESR signals similar to those observed in the concentrated acid. The UV–Vis spectrum of a 4×10^{-4} M solution initially showed the presence of the aqua ion **2** and an absorption at 488 nm (**3**, possibly with some coordinated chloride) which decreased so that **2** was the only species present after about 1.5 h.

A 4×10^{-4} M solution of $Cs_2[TcNCl_5]$ in 5 M $MeSO_3H$ showed different behaviour. The initial UV–Vis spectrum of the pink solution (Fig. 4) did not show the presence of a significant amount of $[TcNCl_4]^-$ but an absorption maximum at 497 nm which increased ($\epsilon > 4800$, for a dimer) and then after ~30 min began to decrease. The strong visible absorption suggests a derivative of the μ-oxo dimer **3** with some of the coordinated waters replaced by chloride. After ~3 h the presence of the di(μ-oxo) cation **2** became apparent. A 2×10^{-3} M solution showed a maximum at 515 nm (due to a greater number of coordinated chlorides than in the 497 nm species). Addition of CF_3SO_3Ag to this solution resulted in an orange colour and a shift in the absorption maximum to 477 nm due to the formation of a mixture of the aqua ions **2** and **3** (Fig. 4). This confirms the presence of coordinated chloride in the 515 and 497 nm species and supports the formulations as derivatives of the singly oxygen-bridged **3**. It may be noted that, as expected, in the presence of a limited amount of chloride this anion preferentially complexes to the more highly charged aqua cation. An absorption at 540 nm has been reported for the pink solution of $Cs_2[TcNCl_5]$ in 0.5 M HCl and it was suggested that this might be due to $[Tc_2N_2O_2Cl_4]^{2-}$ [20]. We have since isolated the yellow $(AsPh_4)_2[Tc_2N_2O_2Cl_4]$ and thus it seems that the 540 nm species in 0.5 M HCl should be formulated as a chloro derivative of **3**, with the bathochromic shift indicating coordination by a greater number of chloro ligands than in the 497 nm species in 5 M $MeSO_3H$. The behaviour of $Cs_2[TcNCl_5]$ in 1 M $MeSO_3H$ paralleled that in 1 M CF_3SO_3H with the absorption maximum at 497 nm decreasing and only the spectrum of **2** remaining after about 5 h. The ESR spectrum of $Cs_2[TcNCl_5]$ in 1 M $MeSO_3H$ was poorly resolved and corresponded in intensity to only ~5% of the Tc present. The spectrum was similar to that of $Cs_2[TcNCl_5]$ in 1 M CF_3SO_3H.

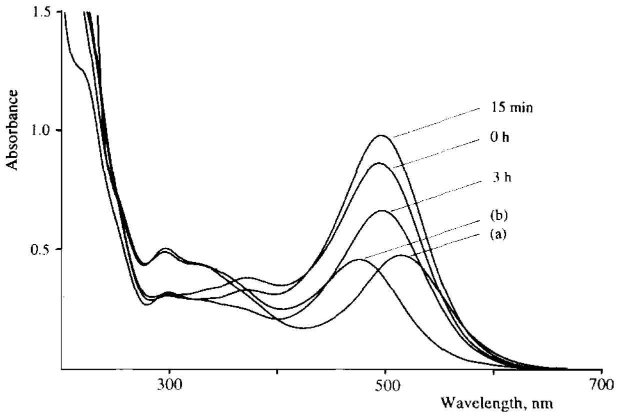

Fig. 4. UV–Vis spectra of 4×10^{-4} M $Cs_2[TcNCl_5]$ in 5 M $MeSO_3H$ showing the 497 nm species at preparation and after 15 min and 3 h. Spectrum (a) is of a 2×10^{-3} M solution after 23 h showing the 515 nm species. Spectrum (b) shows the conversion to **3** (477 nm) after the addition of solid CF_3SO_3Ag and removal of AgCl (2 mm cell).

Hpts is less suitable for optical studies since the strong absorption of the acid limits the wavelength range to above ~300 nm. A 2×10^{-3} M solution of **1** in 4 M Hpts showed the presence of **2** and **3** after 15 h. A 4×10^{-4} M solution of $Cs_2[TcNCl_5]$ was purple–pink and showed an absorption maximum at 500 nm which decreased on standing by a factor of 2.4 after 3.5 h. A 2×10^{-3} M solution showed a maximum at 519 nm due to a chloro derivative of **3** with more coordinated chloride than the 500 nm species, which decreased by a factor of only 0.9 between 7.5 h and 29 h. Addition of Agpts at both times again gave orange solutions with maxima at 477 due to **3**. Solutions of **1** and $Cs_2[TcNCl_5]$ in 1 M Hpts contained only **2** after 30 min.

Solutions of $Cs_2[TcNCl_5]$ in 2 M Hpts gave, when frozen immediately, ESR signals corresponding in intensity to ~15% of the Tc present. The ESR spectral parameters for the species observed in 2 M Hpts are given in Table 1 and are similar to those for $Cs_2[TcNCl_5]$ in anhydrous CF_3SO_3H. No signals were observed from this solution when frozen after standing at room temperature for 20 min or from a solution of $Cs_2[TcNCl_5]$ in 0.25 M Hpts when frozen immediately after preparation.

Electrophoretic studies have previously shown that in 0.5 M CF_3SO_3H, $MeSO_3H$ and Hpts solutions of **1** all the technetium is present as the cationic species **2** [4]. The lability of the chloro ligands in the $Cs_2[TcNCl_5]$ solutions was demonstrated by the electrophoresis of a purple–pink 0.01 M $Cs_2[TcNCl_5]$ solution in 1 M Hpts using 0.5 M Hpts as the electrolyte, when the purple–pink spot on the paper rapidly faded after application of the voltage due to the removal of chloride by migration to the anode and the formation of **2**. The formation of **2**, with no chloride coordination, in 4×10^{-4} M $Cs_2[TcNCl_5]$ solutions in the 0.5 M acids on standing cannot thus be established by electrophoresis but is inferred from the identity of the UV–Vis spectra with those of solutions of **1**.

The above results show that the monomeric $[TcN(OH_2)_5]^{3+}$ ion is not a viable species but dimerises even in strongly acid solution. A similar conclusion was reached by Kim *et al.* for the $[MoO(OH_2)_5]^{3+}$ ion [21]. These authors found a Mo_2O_3 dimeric species to be the major form in 12 M $MeSO_3H$. We note that a $[Mo_2O_3(OH_2)_n]^{4+}$ ion has not been identified [19] or, it would appear, claimed. A variety of transition metal trifluoromethanesulfonate complexes have been prepared, usually by the treatment of a halide with the anhydrous acid and removal of HCl. These complexes undergo rapid and complete aquation in water [22]. It is thus reasonable to assign the 474 nm absorption of solutions of **1** in 7.5 M CF_3SO_3H to the aquanitrido cation **3** since the very weakly nucleophilic $CF_3SO_3^-$ anion is not expected to compete effectively with water for coordination sites. For $Cs_2[TcNCl_5]$ solutions the monomeric form is stabilised by chloride coordination and the sequence monomer → μ-oxo dimer → di(μ-oxo) dimer is time and acid concentration dependent, with the complete conversion to **2** occurring in the dilute acids.

Studies in sulfuric acid

Sulfuric acid is a better complexing medium than sulfonic acids, with the HSO_4^- anion acting as the ligand at higher concentrations and SO_4^{2-} in more dilute solution. The UV–Vis spectra of solutions of **1** in the 98% and 10 M acids are shown in Fig. 5. In the 98% acid, a solution of **1** was initially a pale cherry colour which rapidly faded to give the monomeric form $[TcN(HSO_4)_n]^{(n-3)-}$ ($n = 4$ or 5) (λ_{max} 296 nm, $\epsilon \sim 3800$, for a monomer) and then showed little change over 6 h. In 10 M H_2SO_4 a solution of **1** was orange and showed a maximum at 485 nm ($\epsilon > 6700$, for a dimer) which is assigned to the μ-oxo species **4** with SO_4^{2-} coordination (*vide infra*).

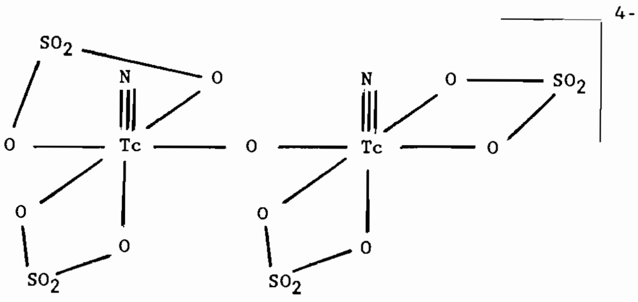

4

Addition of solid Ag_2SO_4 to the solution did not affect the intensity of the 485 nm peak, indicating that **4** is not oxidised by Ag^+. In 5 M H_2SO_4 the absorption at 485 nm was initially weak but increased by a factor of 9 over 24 h ($\epsilon > 9000$, for a dimer). In 2 and 1 M H_2SO_4 the absorbance at 486 nm increased on standing with the greater relative increase in the 2 M case (ϵ 2700, for a dimer after 3 days). The presence of a spectrum indistinguishable from that of **2** was also apparent. The absence of coordinated SO_4^{2-} cannot, however, be assumed since it is noted that the UV–Vis spectrum of $[Mo_2O_4(edta)]^{2-}$ (edta = ethylenediaminetetraacetate(4 −)) is similar in appearance but enhanced in intensity relative to that of the $[Mo_2O_4(OH_2)_6]^{2+}$ cation [19]. In 0.25 M H_2SO_4 only the **2**-like spectrum was observed after 10 h.

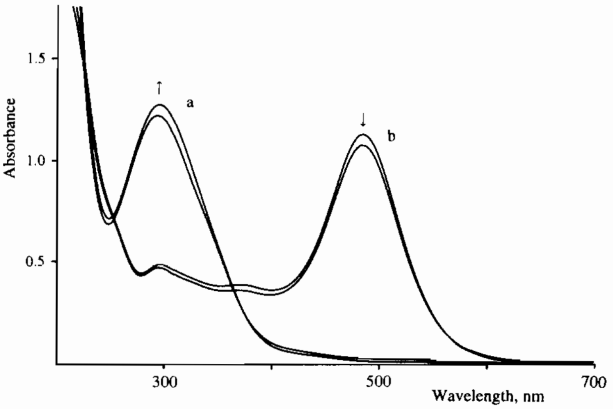

Fig. 5. UV–Vis spectra of: (a) **1** in conc. H_2SO_4 ($[Tc] = 3.32 \times 10^{-4}$ M) at preparation and after 6 h; (b) **1** in 10 M H_2SO_4 ($[Tc] = 8.25 \times 10^{-4}$ M) at preparation and after 9.5 h.

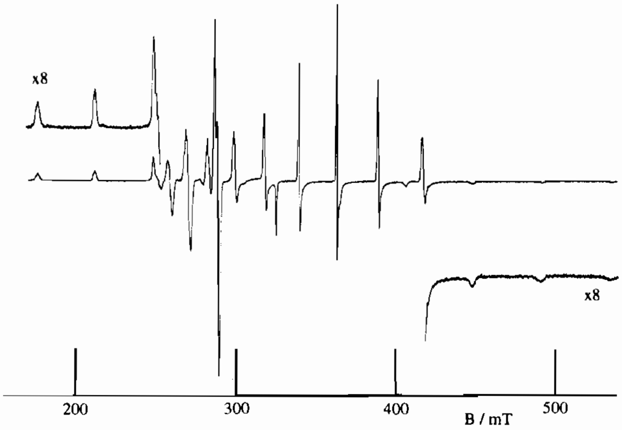

Fig. 6. ESR spectrum of **1** in conc H_2SO_4 ($[Tc] = 1.66 \times 10^{-3}$ M) and frozen to 130 K after 10 min at room temperature. Spectrometer conditions: microwave frequency, 9.513 GHz; microwave power 2.0 mW; 100 kHz modulation amplitude 0.2 mT; spectrometer gain 4.0×10^4; recorder time constant 0.1 s; scan rate 0.8 mT/s.

The ESR spectrum of **1** in 98% H_2SO_4, examined during the first few hours after preparation, gave evidence for the presence of a number of species with similar spin Hamiltonian parameters (Figs. 6 and 7). The interpretation of the spectrum is complicated because of species with different linewidths and the appearance of superhyperfine structure on some of the perpendicular features. Whilst definitive identification could not be made, the superhyperfine effects are best explained as arising from coordination of HSO_4^- via oxygen but where there is sufficient electron delocalisation to give the small ($\sim 2.5 \times 10^{-4}$ cm^{-1}) splitting observed. A much simpler spectrum, due to a single species which exhibited no superhyperfine structure,

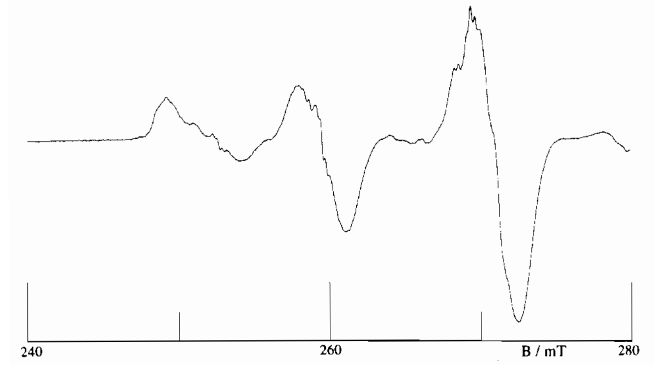

Fig. 7. Expansion of part of Fig. 6, to show the presence of more than one species and superhyperfine structure. Spectrometer conditions as for Fig. 6 apart from gain (10×10^4) and scan rate (0.2 mT/s).

was observed from solutions which had been standing at room temperature for some days. The spin Hamiltonian parameters, given in Table 2, are consistent with coordination to HSO_4^- and are almost identical to those derived for the freshly frozen solutions. It is possible that the differences in resolution between solutions frozen immediately and those left standing for some days are due to changes in the glass-forming behaviour of the solvent with time, as well as to small chemical changes.

The ESR spectrum of solutions of **1** in 10 M H_2SO_4 examined within a few minutes after preparation showed the presence of only one species which accounted for only about 1% of the Tc present. The spectral intensity increased on standing at room temperature and after 24 h accounted for most of the Tc present. Similarly, only weak signals were observed from 5, 1 and 0.25 M H_2SO_4 solutions. However, the signal intensity increased on standing although even in the 5 M solution the intensity after 24 h accounted for only about 10% of the Tc present. The ESR spectral parameters of the species observed in the 10 M and weaker H_2SO_4 solutions are given in Table 2. The spectral parameters are different to those found for the species in conc. H_2SO_4 and are consistent with the coordination of SO_4^{2-}.

The time and acid concentration dependence of the UV–Vis and ESR spectra of $Cs_2[TcNCl_5]$ in H_2SO_4 solutions reflects the competition for coordination to the TcN^{3+} cores by the ligands Cl^-, SO_4^{2-}, HSO_4^-, H_2O and the tendency to form μ-oxo or di(μ-oxo) dimers.

The UV–Vis spectrum of $Cs_2[TcNCl_5]$ in 98% H_2SO_4 showed a complex time dependent behaviour with shifts in absorption maxima as well as intensity. The major absorption maxima occurred at ~290, 316, 360, 405 and 420 nm. A solution in 10 M H_2SO_4 was bright yellow with a single absorption maximum at 355 nm (ϵ 2800, based on a monomeric form). The spectrum was essentially unchanged after 15 h. In 5 M H_2SO_4 (Fig. 8) the absorbance at 487 nm (species **4**) increased for up to about 16 h (ϵ 8600, for a dimer) and then decreased while the absorbance at 344 nm decreased. An isosbestic point at 396 nm indicates the direct conversion of the 344 nm species to **4**. In 2, 1, 0.5 and 0.25 M H_2SO_4 the spectra of the $Cs_2[TcNCl_5]$ solutions were similar to solutions of **1**, with no evidence of chloride coordination. The absorption at 484 nm of the $Cs_2[TcNCl_5]$ solution in 2 M H_2SO_4 showed an increase and then a decrease but in the 1, 0.5 and 0.25 M H_2SO_4 solutions only a decrease was observed. In the 0.25 M H_2SO_4 solution only a **2**-like spectrum was observed after about 17 h. A solution of $Cs_2[TcNCl_5]$

TABLE 2. ESR spectral parameters for sulfuric acid solutions

System	$g_\parallel$ (±0.001)	$g_\perp$ (±0.002)	$A_\parallel$ (±1.0)	$A_\perp$ (±1.0)	Q (±1.0)	Lowest field ∥ lines
			($\times 10^4$ cm^{-1})			
Solutions of 1 in						
Conc. H_2SO_4	(a) 1.900	2.000	353	170	4.0	1755
(immediate)	(b) 1.900	2.000	355	170	4.0	1765
(on standing)	1.898	1.995	355	170	4.0	1760
≤10 M H_2SO_4	1.910	1.990	344	163	4.0	1797
1 M $KHSO_4$	no signals					
Solutions of $Cs_2[TcNCl_5]$ in						
≤10 M H_2SO_4	(a) 1.910	1.987	345	165	4.0	1800
	(b) 1.940	1.990	331	152	4.0	1840
	(c) 1.980	2.001	315	147	4.0	1895
	(d) 1.990	2.002	305	147	4.0	1920
1 M $KHSO_4$	1.910	1.988	344	163	4.0	1800

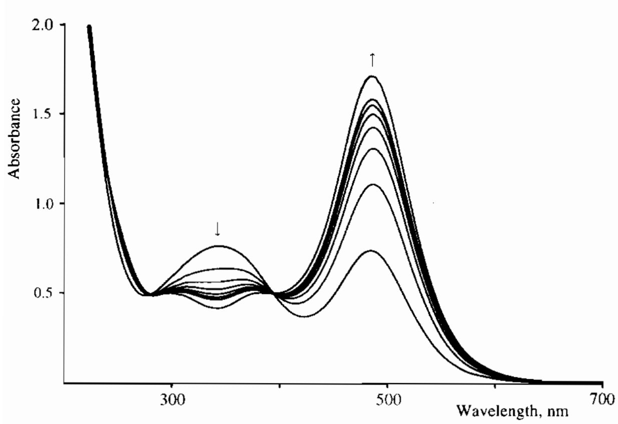

Fig. 8. UV–Vis spectra of 4×10^{-4} M $Cs_2[TcNCl_5]$ in 5 M H_2SO_4 at preparation and at 30 min intervals for up to 3 h and then at 9.5 h.

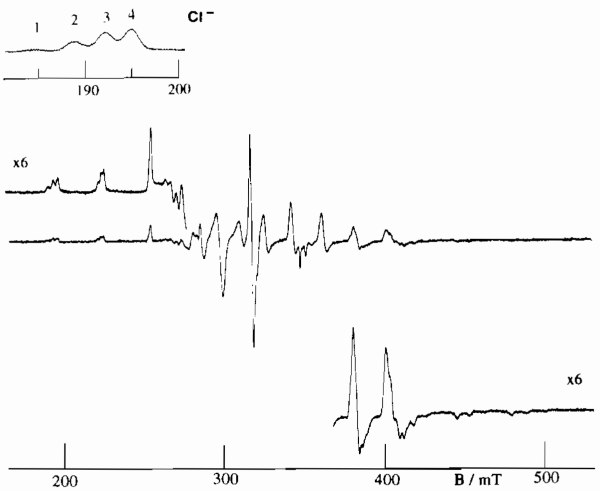

Fig. 9. ESR spectrum of 2.0×10^{-3} M $Cs_2[TcNCl_5]$ in 10 M H_2SO_4 and frozen to 130 K. Spectrometer conditions: microwave frequency, 9.513 GHz; microwave power 2.0 mW; 100 kHz modulation amplitude 0.1 mT; spectrometer gain 8×10^4; recorder time constant 0.1 s; scan rate 0.8 mT/s. The inset shows an expanded view of the lowest field parallel lines due to the species with 4, 3, 2 and 1 coordinated chloride ions at 195, 192, 189 and 185 mT, respectively.

in 1 M $KHSO_4$ showed very similar behaviour to a solution in 0.5 M H_2SO_4.

The nature of the 484 nm and **2**-like species was clarified by the electrophoresis of a 0.02 M solution of $Cs_2[TcNCl_5]$ in 0.5 M H_2SO_4 using the same concentration of acid as the electrolyte. When the electrophoresis was performed shortly after the dissolution of the $Cs_2[TcNCl_5]$, the Tc radioactivity was separated as a colourless cation (~55%) at ~1 cm from the origin and an orange anion with about the same (but opposite) migration. After 24 h the cation accounted for ~82% of the Tc. Under the same conditions in 0.5 M CF_3SO_3H the aqua cation **2** migrates about 4 cm. The cationic species in 0.5 M H_2SO_4 thus appears to be **2** partially coordinated to SO_4^{2-} or a mixture of **2** and other cationic, neutral or anionic species which undergo ligand exchange rapidly relative to the separation time and thus exhibit average behaviour corresponding to a net positive charge. The orange anionic species is thus the μ-oxo dimer coordinated by, on average, at least three SO_4^{2-} anions. That the sulfate is only weakly bound was shown by electrophoresis of the $Cs_2[TcNCl_5]$ solution in 0.5 M H_2SO_4 (at 1 h after preparation) using 0.5 M Hpts as the supporting electrolyte, when only the cation **2** was observed.

The ESR spectrum of $Cs_2[TcNCl_5]$ in 98% H_2SO_4 exhibited signals which are attributed to the replacement of one or more chloro ligands by HSO_4^-. The signals due to $[TcNCl_4]^-$ contained only about 5% of the total intensity, which corresponded to all of the Tc present. The overall spectral intensity did not change with time. In the 10 M acid the most prominent signal was that due to $[TcNCl_4]^-$, corresponding to about 40% of the total signal intensity (Fig. 9). The remaining three species could be attributed to the replacement of one, two or three chloro ligands by SO_4^{2-}. The total signal intensity did not change over 5 days, and again corresponded to all the Tc present in solution. In the 5 M acid, only three species were observed, attributed to coordination of none, one and two chloride ligands with the remaining positions being occupied by SO_4^{2-}. The initial signal intensity corresponded to all the Tc present but decreased to about 40% of the initial value after 5 days at room temperature. Only two species were observed in 2.5 M acid and only one in 1 M acid at preparation. The overall signal intensity was much reduced in both cases. No signals were observed from a 0.25 M solution or from 2.5 and 1 M solutions after standing for 5 days at room temperature, but the full signal intensity, in the form of $[TcNCl_4]^-$, was restored by the addition of an equal volume of conc. HCl.

The ESR spectra of **1** and $Cs_2[TcNCl_5]$ in 1 M $KHSO_4$ were also studied. Only weak signals were observed from solutions of **1** when frozen within 5 min of preparation. Solutions of $Cs_2[TcNCl_5]$ also only gave relatively weak signals corresponding in intensity to about 2% of the Tc present and which appeared to be similar to those observed in 2 M H_2SO_4. These signals disappeared after the solutions were allowed to stand for 4 h at room temperature.

Our results for $Tc^{VI}N$ in H_2SO_4 are consistent with the magnetic and UV–Vis studies of Rudolf and Wolniak [23] and the ESR studies of Marov *et al.* for Mo^VO in H_2SO_4 [24]. The first authors found that the mean magnetic moment of the Mo^V ion decreased from 1.702 to 0.312 BM as the H_2SO_4 concentration was decreased from 15.4 to 6.9 M, a result consistent with an increase in the concentration of diamagnetic dimeric forms. A strong absorption at 410 nm in the electronic spectrum was ascribed to the μ-oxo dimer $[Mo_2O_3(HSO_4)_6(OH_2)_2]^{2-}$.

Studies in sulfamic and other acids

The reported preparation of a number of sulfamato complexes of Rh, Ir, Ru and Os in aqueous solution suggested that this acid might coordinate to $Tc^{VI}N$ [25]. The UV–Vis spectrum of a solution of $Cs_2[TcNCl_5]$ in 1 M NH_2SO_3H, however, showed the presence of only the di(μ-oxo) aqua cation **2** after 15 min. The presence of **2** was confirmed by electrophoresis. These results show that NH_2SO_3H is, like RSO_3H, essentially non-complexing towards $Tc^{VI}N$. The low aqueous solubility of the zwitterionic $NH_2CH_2SO_3H$ and pyridine-3-sulfonic acid preclude any useful comparisons with these acids. A solution of **1** in 1 M 3-carboxy-4-hydroxybenzenesulfonic acid, which contains both a carboxylic acid and phenolic group, was pale pink and showed an absorption at 502 nm which increased by a factor of 2 after 4 days ($\epsilon \sim 1100$, for a dimer). A solution of $Cs_2[TcNCl_5]$ in the 1 M acid gave an initial strong absorption at 504 nm (ϵ 7000, for a dimer) which reduced by a factor of 4.4 after 21 h. The presence of the additional complexing groups thus stabilise the μ-oxo species.

Studies in phosphorus oxo acids

The behaviour of **1** and $Cs_2[TcNCl_5]$ in phosphoric acid solutions reflects the greater coordinating ability of these media in comparison with H_2SO_4. The reaction sequence is proposed where $L = H_2PO_4^-$, $L_2 = HPO_4^{2-}$ or $L_3 = PO_4^{3-}$, depending on the acidity.

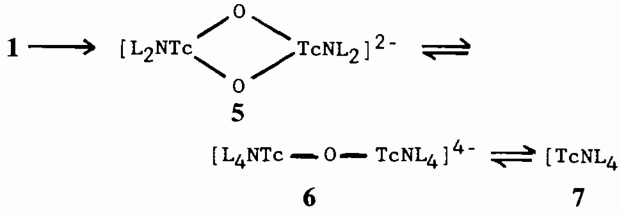

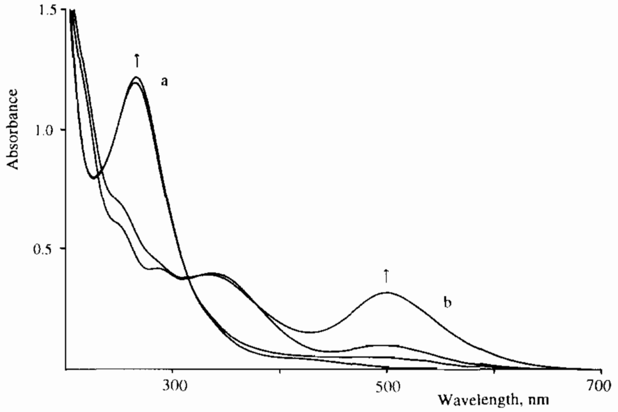

Fig. 10. UV–Vis spectra of: (a) **1** in 17.5 M H_3PO_4 ($[Tc] = 2.77 \times 10^{-4}$ M) at preparation and after 3 h; (b) **1** in 0.25 M H_3PO_4 ($[Tc] = 3.28 \times 10^{-4}$ M) at preparation and after 16 h.

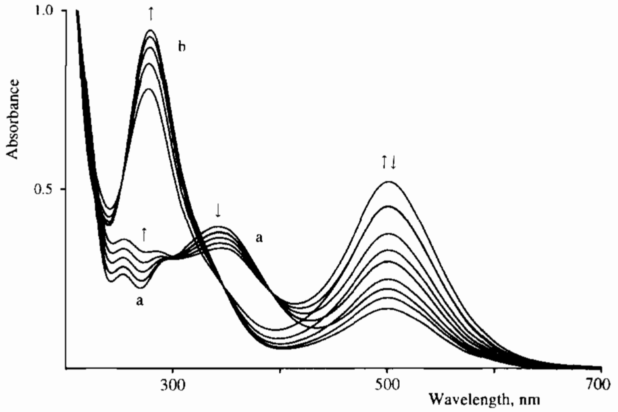

Fig. 11. UV–Vis spectra of **1** in 5 M H_3PO_4 ($[Tc] = 3.24 \times 10^{-4}$ M): (a) at preparation and 15, 30, 45 and 60 min; (b) at 19, 21, 23, 25 and 27 h.

The changes in composition were readily followed by optical spectroscopy. A solution of **1** in 17.5 M H_3PO_4 was briefly a pale cherry colour and then became almost colourless. The UV–Vis spectrum (Fig. 10) showed a single absorption at 266 nm ($\epsilon > 4400$) which is assigned to the monomer **7** with $L = H_2PO_4^-$. In 0.25 M H_3PO_4 (Fig. 10) the absorptions at ~336 and 500 nm are assigned to **5** and **6**, respectively. The reaction sequence **5**→**6**→**7** is nicely observed in 5 M H_3PO_4 (Fig. 11). During the first hour the fast reaction **5**→**6** is predominant and results in the isosbestic points at 299 and 394 nm. After about 19 h the predominant reaction is **6**→**7**, with isosbestic points at 253 and 347 nm. In 10 M H_3PO_4 the same sequence occurred more rapidly, with the absorption at 500 nm (responsible for the purplish colour of the solution) first increasing and then decreasing until after about 11 h only the spectrum of **7** remained. A solution of **1** in 1 M H_3PO_4 showed only evidence for **5**→**6** with the absorbance 500 nm continuing to increase at up to 15 h.

$Cs_2[TcNCl_5]$ proved difficult to dissolve in the higher concentrations of H_3PO_4, but in the 2 M acid the $[TcNCl_4]^-$ anion was rapidly converted to the monomeric form **7**. The conversion of **7** to the μ-oxo dimer **6** was demonstrated by the decrease in the peak at 273 nm and the increase in the 500 nm peak. In 0.5 and 0.25 M H_3PO_4 the spectra showed no evidence of the initial presence of **7**, indicating rapid formation of **6** which then slowly converted to **5**. The initial absorption at 500 nm was reduced after 15 h by a factor of 1.2 for the 0.5 M and 2 for the 0.25 M acid. Similar behaviour was observed in 1 M NaH_2PO_4 (pH 4.1) and the alkaline 1 M K_2HPO_4 (pH 9.5), with the peaks at 505 and 508 nm, respectively, decreasing by factors of 3 and 8.5 after 1.5 h. The isosbestic points at 290 and

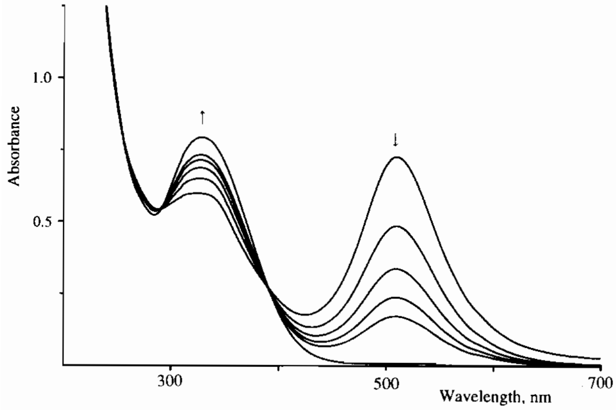

Fig. 12. UV–Vis spectra of 4×10^{-4} M $Cs_2[TcNCl_5]$ in 1 M K_2HPO_4 at preparation, 15, 30, 45, 60 min and 11 h.

390 nm in the spectra of the K_2HPO_4 solution (Fig. 12) show that the 508 nm species is converted directly to a yellow 327 nm species which appears related to the 344 nm species reported for a solution of **1** in 0.1 M CsOH [4]. Electrophoresis of a freshly prepared solution of $Cs_2[TcNCl_5]$ in 0.5 M H_3PO_4 (1000 V, 40 min) gave an anionic purple–pink spot at ~2 cm. The slow migration indicated that, even allowing for greater ionic size, the highly charged anion **6** was not the major component under these conditions. After 24 h electrophoresis showed the presence of three species one at the origin and two anionic species at ~2 and 3.5 cm.

Solutions of **1** and $Cs_2[TcNCl_5]$ in 2 M H_3PO_3 showed similar UV–Vis spectral behaviour to the respective solutions in H_3PO_4. The stability of monomeric $Tc^{VI}N$ in aqueous H_3PO_3, a fairly strong reducing agent, is surprising in view of the ease of reduction of $[TcNCl_4]^-$ in organic solvents [14].

The ESR spectra of **1** and $Cs_2[TcNCl_5]$ in phosphorus oxo acid solutions give direct evidence for coordination by different types of phosphorus oxo anions. Thus, in 17.5 M phosphoric acid the coordinating species is expected to be $H_2PO_4^-$, in dilute phosphoric acid HPO_4^{2-} or PO_4^{3-}, in phosphorous acid $H_2PO_3^-$ or HPO_3^{2-} and in pyrophosphoric acid $H_2P_2O_7^{2-}$. These differences in coordination are reflected in the differences in the ESR spectral parameters given in Table 3. Where the spectral parameters for different solutions are closely similar, it should be noted that the simulations are influenced by linewidth considerations and that differences between the values of $A_{\parallel}$ are better indicators than those between $g_{\parallel}$. It should also be noted that it is more difficult to determine $g_{\perp}$, $A_{\perp}$ and Q than to determine $g_{\parallel}$ and $A_{\parallel}$.

The ESR spectrum of **1** in 17.5 M H_3PO_4 showed only the single species **7** (Fig. 13). The spin Hamiltonian parameters are given in Table 3. The spectral intensity increased by a factor of about 2.5 after standing for some days. No signals were observed from solutions of **1** in 10, 5 and 0.25 M H_3PO_4 immediately after preparation. However, signals did develop in the first two solutions after standing for three days at room temperature. The ESR spectral parameters of the single species observed are given in Table 3 and are seen to differ in detail from those for the concentrated acid. The difference is presumably due to coordination by $H_2PO_4^-$ in concentrated acid and by HPO_4^{2-} or PO_4^{3-} in the more dilute acid solutions. A solution of **1** in 2 M H_3PO_3 frozen immediately after dissolution showed only very weak ESR signals, but these increased by a factor of 25 on standing for 24 h (Fig. 14). The signal intensity decreased after several more days presumably due to the slow reduction of $Tc^{VI}N$ to $Tc^{V}N$. The initial spectral intensity of $Cs_2[TcNCl_5]$ in 2 M H_3PO_3 accounted for most of the Tc present and decreased by a factor of ~5 after standing for 24 h at room temperature. The same species was observed at both times and the spin Hamiltonian parameters are given in Table 3. These differ in detail from those for H_3PO_4 solutions as shown by an examination of the region around 300 mT (Figs. 13 and 14), and indicate that the coordinating species is a phosphite anion.

Solutions of **1** and $Cs_2[TcNCl_5]$ in 1 M $H_4P_2O_7$ showed similar behaviour to the 1 M H_3PO_4 solutions. Solutions of **1** in 2 M $H_4P_2O_7$ initially exhibited no ESR signals. However, signals developed on standing and after 4 days accounted for most of the Tc present. The ESR spectral parameters are given in Table 3. Solutions of $Cs_2[TcNCl_5]$ in 2 M $H_4P_2O_7$ exhibited ESR signals corresponding in intensity to most of the Tc present. The spectral parameters (Table 3) indicate the formation of species with pyrophosphate coordination. The spectrum changed on standing and after 4 days was similar to that of $Cs_2[TcNCl_5]$ in 2 M H_3PO_4. This is presumably due to the slow hydrolysis of $H_4P_2O_7$ to H_3PO_4 and coordination by phosphate ligands.

Recovery studies

The stability of $Tc^{VI}N$ in acid solutions was confirmed by the recovery of $AsPh_4[TcNCl_4]$ (identified by m.p. and IR spectroscopy [5]) after treatment with conc. HCl and precipitation by $AsPh_4Cl$. For $Cs_2[TcNCl_5]$ in 98% H_2SO_4, 92% of the Tc was recovered as $AsPh_4[TcNCl_4]$ after 5 h and for **1** in 10 M H_2SO_4, 98% after 30 days. Similarly for **1** in 17.5 M H_3PO_4, 98.3% was recovered after 24 h and for $Cs_2[TcNCl_5]$ in 0.25 M H_3PO_4 the recovery was 83% after 38 days. From a solution of **1** in 7.5 M CH_3SO_3H only 40% of the Tc was recovered after 3 months. It was, however, noted that on prolonged standing in acid solutions some of the TcN^{3+} is converted to a form which does not form $[TcNCl_4]^-$ on addition of HCl. This was demonstrated by the addition of H_2O_2 to the filtrate (after

TABLE 3. ESR spectral parameters for phosphorus oxo acid solutions

System	$g_{\parallel}$ (±0.002)	$g_{\perp}$ (±0.003)	$A_{\parallel}$ (±1.0)	$A_{\perp}$ (±1.0)	Q (±1.0)	Lowest field ∥ lines
			($\times 10^4$ cm^{-1})			
Solutions of 1 in						
17.5 M H_3PO_4	1.904	1.990	353.2	168	3.5	1764
10 and 5 M H_3PO_4	1.905	1.990	349	165	3.0	1780
2 M H_3PO_3 (after 24 h)	1.909	1.986	347	164	4.0	1790
2 M $H_4P_2O_7$ (after 4 days)	1.905	1.985	348	165	3.0	1785
Solutions of $Cs_2[TcNCl_5]$ in						
2 M H_3PO_3	1.909	1.986	347	164	4.0	1790
2 M $H_4P_2O_7$						
(immediate)	1.912	1.985	344	162	3.0	1800
(on standing)	1.905	1.985	348	165	3.0	1785

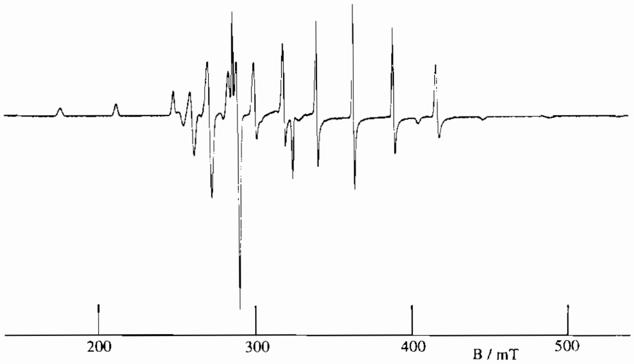

Fig. 13. ESR spectrum of 1 in 17.5 M H_3PO_4 ([Tc] = 1.4×10^{-3} M), frozen to 130 K 24 h after mixing. Spectrometer conditions: microwave frequency, 9.513 GHz; microwave power 2.0 mW; 100 kHz modulation amplitude 0.4 mT; spectrometer gain, 2.5×10^4; recorder time constant 0.05 s; scan rate 2.0 mT/s.

removal of $AsPh_4[TcNCl_4]$) when a tan precipitate formed which after drying was converted to a mixture of $AsPh_4[TcNCl_4]$ and $(AsPh_4)_2[TcCl_6]$ on dissolution in $SOCl_2$.

UV–Vis spectra of $Tc^{VI}N$ complexes

A characteristic feature of $Tc^{VI}N^{3+}$ non-chloro monomeric species is a strong absorption at 266–300 nm (Table 4) which is assigned to a $\pi N \rightarrow Tc$ charge transfer transition. In the case of $[MoOL_4]^-$ (L = $H_2PO_4^-$ or HSO_4^-) the spectra show a featureless increase in intensity from about 330 to 200 nm [27] indicating that the $\pi O \rightarrow Mo$ transition occurs at higher energy [28] than the analogous $\pi N \rightarrow Tc$ transition. The spectra of $Cs_2[TcNCl_5]$ in 7.5 M HCl (Fig. 1) and $(NH_4)_2[MoOCl_5]$ in 10 M HCl [29] are similar in shape (and except for the highest energy peak, similar in intensity) but with the peaks shifted to lower energies for $[TcNCl_4]^-$ (Table 4). The 399 nm peak and the shoulder at 480 nm for $[TcNCl_4]^-$ are assigned to $\pi Cl \rightarrow Tc$ charge transfer transitions by analogy with $[MoOCl_5]^{2-}$ [27, 30].

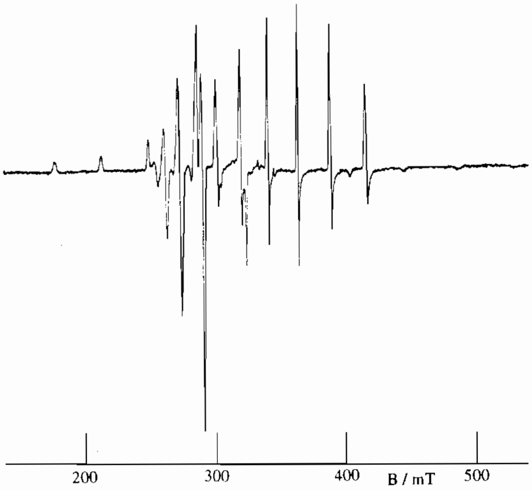

Fig. 14. ESR spectrum of 1 in 2 M H_3PO_3 ([Tc] = 1.45×10^{-3} M) at 130 K. Spectrometer conditions: microwave frequency, 9.523 GHz; microwave power 2.0 mW; 100 kHz modulation amplitude 0.4 mT; spectrometer gain 5.0×10^4; recorder time constant 0.1 s; scan rate 2.0 mT/s.

The intense absorption at 470–510 nm for the $Tc^{VI}N$ μ-oxo dimers containing oxygen ligands clearly does not arise from the mononuclear constituents. Since such a band is not observed for the di(μ-oxo) dimers, and the intensity is inconsistent with a Tc d–d transition, it is assigned to a transition within the a linear (or near linear) Tc–O–Tc three centre π-bond system (Tc–O bond order 1.5) as has been suggested for Mo^VO μ-oxo dimers [1]. For Mo^VO in H_2SO_4 the μ-oxo dimer absorbs at 410 nm [23] while for Tc^VN the absorption is lower in energy at 485 nm. The spectrum of 2 is

TABLE 4. UV–Vis spectra of $Tc^{VI}N$ complexes

System	λ_{max} (nm)	(ϵ (M^{-1} cm^{-1}))
$Cs_2[TcNCl_5]$ in 7.5 M HCl	293	(1535)
	399	(4780)
	480sh	(625)
$[MoOCl_5]^{2-}$ in 9-12 M HCl[a]	240	(5500)
	311	(4400)
	355	(500)
Solutions of 1 in		
CF_3SO_3H (anhyd.)	299	(>12700)
H_2SO_4 (98%)	296	(~3800)
17.5 M H_3PO_4	266	(>4400)
Di(μ-oxo) dimer		
$[\{TcN(OH_2)_3\}_2(\mu\text{-}O)_2]^{2+}$ (**2**)		
(in 1 M CF_3SO_3H)	251	(2760)
	295	(2580)
	331sh	(1930)

[a] Data from ref. 26.

similar to that of $[Mo_2O_4(OH_2)_6]^{2+}$, which also shows absorption maxima at 255 (ϵ 4320) and 295 (ϵ 3550) [31]. However, the shoulder at 331 nm (ϵ 1930) for **2** is much more intense and at higher energy than a corresponding shoulder at 384 nm (ϵ 103) for $[Mo_2O_4(OH_2)_6]^{2+}$.

Comparison of $Tc^{VI}N$ and $MO^{V}O$

The $Tc^{VI}N^{3+}$ ion resembles the isoelectronic $Mo^{V}O^{3+}$ d^1 'yl' ion in many respects, but in particular in the formation of stable monomeric and dimeric μ-oxo and di(μ-oxo) complexes [1]. The monomeric aqua ions $[TcN(OH_2)_5]^{3+}$ and $[MoO(OH_2)_5]^{3+}$ rapidly dimerise even in strong solutions of weakly coordinating acids. For electrochemically generated monomeric $Mo^{V}O(aq)^{3+}$ in 1–2 M CF_3SO_3H, the rate constant for the spontaneous dimerisation has been estimated at 10^3 M^{-1} s^{-1} [32]. It may be noted that the isoelectronic $[V^{IV}O(OH_2)_5]^{2+}$ is stable and appears to show little tendency to dimerise in acid solution [33]. The first $[V^{IV}O\text{–}O\text{–}V^{IV}O]^{2+}$ complex, $[\{(tpa)VO\}_2(\mu\text{-}O)](ClO_4)_2$ (tpa = tri(pyridylmethyl)amine), has only been recently reported [34]. The strong tendency for the $[TcN(OH_2)_5]^{3+}$ and $[MoO(OH_2)_5]^{3+}$ ions to dimerise is no doubt due to the need to reduce the large positive charge and the apparent inability to form monomeric nitridooxo or dioxo species, respectively. The only monomeric compounds of the isoelectronic $Tc^{VI}O^{4+}$ to have been prepared are $(NMe_4)_2[TcO_4]$ [35], $TcOX_4$ (X = F, Cl) [36] and $[TcOCl_5]^-$ [37], all of which rapidly disproportionate in water. An organometallic $Tc^{VI}O$ di(μ-oxo) dimer, $[\{(CH_3)_2TcO\}_2(\mu\text{-}O)_2]$, has recently been reported [38].

A marked difference between $Tc^{VI}N$ and $Mo^{V}O$ is that while solutions of $[MoOCl_5]^{2-}$ in acids appear to reach equilibrium rapidly [18, 21], the core interconversions for $Tc^{VI}N$ are much slower processes. In both cases it is evident that both the acidity and the presence and the nature of coordinating ligands determine which of the monomeric and dimeric forms occur in solution. For 4×10^{-4} M $Cs_2[TcNCl_5]$ solutions in weakly coordinating acids the complete removal of the chloro ligands to form **2** requires low acid concentrations. Cation **2** appears to have lesser affinity for chloride than the more highly charged **3** or monomeric TcN^{3+} at low concentrations. The slow rate of core interconversion for $Tc^{VI}N$ indicates that kinetic control will be important in the preparative chemistry, in particular the use of **1** or $Cs_2[TcNCl_5]$ as starting material may result in the isolation of different products. We are currently investigating this aspect of $Tc^{VI}N$ chemistry.

Oxygen exchange studies have shown that the terminal 'yl' oxo ligands of $[Mo_2O_4(OH_2)_6]^{2+}$ exchange much more rapidly ($t_{1/2}\sim4$ min at 0 °C) than the bridging oxygens ($t_{1/2}\sim100$ h at 40 °C) [39]. A notable feature of the yl oxygen exchange is the acidity independence in the range $[H^+]=0.01\text{–}3.1$ M. In the case of **2** the mechanism which results in the exchange of the yl oxygens on Mo (an internal electron rearrangement has been suggested [40]) is clearly not operative since it would result in the irreversible loss of the nitrido ligand as NH_4^+. Bridging oxygen exchange in $[Mo_2O_4(OH_2)_6]^{2+}$ is dependent on $[H^+]^2$ and requires the breakage and reformation of one (or both) of the oxygen bridges [39]. The slow rate of interconversion of **2** and **3** suggests that the exchange of the bridging oxygens in $[Tc_2N_2O_2(OH_2)_6]^{2+}$ (**2**) is slower than for the bridging oxygens in $[Mo_2O_4(OH_2)_6]^{2+}$. A definitive answer to this question will, however, require oxygen labelling studies.

In conclusion, we note that preliminary results of EXAFS studies from our laboratory have confirmed the formation of μ-oxo and di(μ-oxo) $Tc^{VI}N$ dimers in solution.

References

1 E. I. Stiefel, *Prog. Inorg. Chem., 22* (1977) 1.
2 B. Spivack and Z. Dori, *Coord. Chem. Rev., 17* (1975) 99.
3 C. D. Garner and J. M. Charnock, in G. Wilkinson, R. D. Gillard and J. A. McCleverty (eds.), *Comprehensive Coordination Chemistry,* Vol. 3, Pergamon, Oxford, 1987, p. 1329.
4 J. Baldas, J. F. Boas, J. Bonnyman, S. F. Colmanet and G. A. Williams, *Inorg. Chim. Acta, 179* (1991) 151.
5 J. Baldas, J. F. Boas, J. Bonnyman and G. A. Williams, *J. Chem. Soc., Dalton Trans.,* (1984) 2395.
6 J. Baldas, S. F. Colmanet and G. A. Williams, *Inorg. Chim. Acta, 179* (1991) 189.
7 J. Baldas, S. F. Colmanet and M. F. Mackay, *J. Chem. Soc., Dalton Trans.,* (1988) 1725.

8 J. Baldas, J. F. Boas, S. F. Colmanet and G. A. Williams, *J. Chem. Soc., Dalton Trans.,* (1992) 2845.

9 M. R. A. Pillai, C. S. John, J. M. Lo, E. O. Schlemper and D. E. Troutner, *Inorg. Chem., 29* (1990) 1850.

10 J. Baldas and J. Bonnyman, *Int. J. Appl. Radiat. Isot., 36* (1985) 133.

11 J. Baldas, J. F. Boas, J. Bonnyman, S. F. Colmanet and G. A. Williams, *J. Chem. Soc., Chem. Commun.,* (1990) 1163.

12 M. Ardon and A. Pernick, *Inorg. Chem., 12* (1973) 2484.

13 K. Köhler, R. Kirmse and U. Abram, *Z. Anorg. Allg. Chem., 600* (1991) 83.

14 J. Baldas, J. Bonnyman and G. A. Williams, *Inorg. Chem., 25* (1986) 150; J. Baldas and S. F. Colmanet, *Inorg. Chim. Acta, 176* (1990) 1.

15 J. Baldas, J. F. Boas and J. Bonnyman, *Aust. J. Chem., 42* (1989) 639.

16 J. Baldas, J. F. Boas and J. Bonnyman, *J. Chem. Soc., Dalton Trans.,* (1987) 1721.

17 J. A. Craig, E. W. Harlan, B. S. Snyder, M. A. Whitener and R. H. Holm, *Inorg. Chem., 28* (1989) 2082.

18 G. P. Haight, Jr., *J. Inorg. Nucl. Chem., 24* (1962) 663.

19 A. G. Sykes, in G. Wilkinson, R. D. Gillard and J. A. McCleverty (eds.), *Comprehensive Coordination Chemistry,* Vol. 3, Pergamon, Oxford, 1987, p. 1229.

20 J. Baldas and J. F. Boas, *J. Chem. Soc., Dalton Trans.,* (1988) 2585.

21 C.-S. Kim, R. K. Murmann and E. O. Schlemper, *Transition Met. Chem., 9* (1984) 260.

22 G. A. Lawrence, *Chem. Rev., 86* (1986) 17.

23 M. F. Rudolf and A. Wolniak, *Z. Anorg. Allg. Chem., 408* (1974) 214.

24 I. N. Marov, Yu. N. Dubrov, A. N. Ermakov and G. N. Martynova, *Russ. J. Inorg. Chem., (Engl. Transl.), 15* (1970) 1387.

25 W. P. Griffith and D. Pawson, *J. Chem. Soc., Dalton Trans.,* (1973) 524.

26 C. K. Jørgensen, *Acta Chem. Scand., 11* (1957) 73.

27 J. R. Winkler and H. B. Gray, *Comments Inorg. Chem., 1* (1981) 257.

28 H. So and M. T. Pope, *Inorg. Chem., 6* (1972) 1441.

29 H. B. Gray and C. R. Hare, *Inorg. Chem., 1* (1962) 363.

30 M. Brorson and A. Hazell, *Acta Chem. Scand., 45* (1991) 758: D. Collison, *J. Chem. Soc., Dalton Trans.,* (1990) 2999.

31 Y. Sasaki and A. G. Sykes, *J. Chem. Soc., Dalton Trans.,* (1974) 1468.

32 M. T. Paffett and F. C. Anson, *Inorg. Chem., 20* (1981) 3967.

33 L. V. Boas and J. C. Pessoa, in G. Wilkinson, R. D. Gillard and J. A. McCleverty (eds.), *Comprehensive Coordination Chemistry,* Vol. 3, Pergamon, Oxford, 1987, p. 453.

34 H. Toftlund, S. Larsen and K. S. Murray, *Inorg. Chem., 30* (1991) 3964.

35 L. Astheimer and K. Schwochau, *J. Inorg. Nucl. Chem., 38* (1976) 1131.

36 E. Deutsch, K. Libson, S. Jurisson and L. F. Lindoy, *Prog. Inorg. Chem., 30* (1983) 75.

37 R. Kirmse, J. Stach and U. Abram, *Inorg. Chem., 24* (1985) 2196.

38 W. A. Herrmann, R. Alberto, P. Kiprof and F. Baumgärtner, *Angew. Chem., Int. Ed. Engl., 29* (1990) 189.

39 R. K. Murmann, *Inorg. Chem., 19* (1980) 1765.

40 G. D. Hinch, D. E. Wycoff and R. K. Murmann, *Polyhedron, 5* (1986) 487.